

# Axial anomaly in $^3\text{He-A}$ : Simulation of baryogenesis and generation of primordial magnetic field in Manchester and Helsinki.

G.E. Volovik

*Low Temperature Laboratory, Helsinki University of Technology, Box 2200, FIN-02015 HUT, Finland  
and*

*Landau Institute for Theoretical Physics, Moscow, Russia*

(October 19, 2019)

Keywords: superfluid  $^3\text{He}$ , chiral anomaly, gap nodes, effective field theory, effective gravity

The gapless fermionic excitations in superfluid  $^3\text{He-A}$  have the "relativistic" spectrum close to the gap nodes. They are the counterpart of the chiral particles (left-handed and right-handed) in high energy physics above the electroweak transition. The interaction of the chiral fermions with the order parameter give rise to the effect of axial anomaly: conversion of the charge from the coherent motion of the condensate (vacuum) to the quasiparticles (matter). The charge of the quasiparticles is thus not conserved: in other words the matter can be created without creating antimatter. This effect is instrumental for the vortex dynamics, in which the vortex is the mediator of the conversion of the linear momentum from the condensate to the normal component via the spectral flow in the vortex core. The same effect leads to the instability of the counterflow in  $^3\text{He-A}$ , in which the flow of the normal component (incoherent degrees of freedom) is transformed to the order parameter texture (coherent degrees of freedom). We discuss the analogs of these phenomena in high energy physics. The conversion of the momentum from the vortex to the heat bath is equivalent to the nonconservation of baryon number in the presence of textures and cosmic strings. The counterflow instability is equivalent to the generation of the hypermagnetic field via the axial anomaly. We discuss also an analog of axions and different sources of the mass of the "hyperphoton" in  $^3\text{He-A}$ .

## I. INTRODUCTION

### A. Effective electrodynamics and effective gravity in $^3\text{He-A}$ .

Many aspects of the high energy physics can be modelled in condensed matter [1]. In this respect the superfluid  $^3\text{He-A}$  appears to be very useful condensed matter. The most pronounced property of this superfluid is that in addition to the numerous bosonic fields (collective modes of the order parameter) it contains the gapless fermionic quasiparticles. Close to the gap nodes, the points in the momentum space where the energy is zero (Fig. 1), the energy spectrum of quasiparticles is linear in momentum  $\mathbf{p}$ . This simple circumstance has far-reaching consequences: the low energy fermions and some of bosons obey the "relativistic" equations, while their interaction reproduces that of elementary particles with gauge fields. This illustrates the principle [2] that the effective physics in the corner becomes more symmetric than in general. In our case we have two low energy corners with  $\mathbf{p} \approx \pm p_F \hat{\mathbf{l}}$ , where  $p_F$  is the Fermi momentum and  $\hat{\mathbf{l}}$  the unit vector specifying direction of the nodes. This picture does not depend on details of the underlying microscopic interactions of atoms, which only role is to produce the values of the "fundamental constants", such as "speed of light" and "Planck energy".

Close to the gap node the square of the quasiparticle energy  $E$  is generally the quadratic form of the deviation of the momentum  $\mathbf{p}$  from position of the nodes  $\pm p_F \hat{\mathbf{l}}$ :

$$E_{\pm}^2(\mathbf{p}) = g^{ik}(p_i \mp p_F \hat{l}_i)(p_k \mp p_F \hat{l}_k) . \quad (1)$$

Let us introduce the effective vector potential of "electromagnetic field"

$$\mathbf{A} = p_F \hat{\mathbf{l}} , \quad (2)$$

and the "electric charge"  $e$ , with  $e = +1$  for the quasiparticles in the vicinity of the node at  $p_F \hat{\mathbf{l}}$  and  $e = -1$  for the quasiparticles in the vicinity of the opposite node, at  $-p_F \hat{\mathbf{l}}$ . Then one obtains the spectrum of the relativistic fermions moving on the gravitational and electromagnetic fields, determined by the metric tensor  $g^{ik}$  and the vector potential  $\mathbf{A}$ .

$$E^2(\mathbf{p}) = g^{ik}(p_i - eA_i)(p_k - eA_k) . \quad (3)$$

The symmetric matrix  $g^{ik}$  is generally determined by the directions of principal axes forming the orthonormal basis  $(\hat{\mathbf{e}}_1, \hat{\mathbf{e}}_2, \hat{\mathbf{e}}_3)$  and by the "speeds of light" along these directions:

$$g^{ik} = c_1^2 \hat{e}_1^i \hat{e}_1^k + c_2^2 \hat{e}_2^i \hat{e}_2^k + c_3^2 \hat{e}_3^i \hat{e}_3^k . \quad (4)$$

It is important that the effective gauge field  $\mathbf{A}$  and the effective metric  $g^{ik}$  depend on space and time, since the order parameter in general and the  $\hat{\mathbf{l}}$ -vector in particular are not fixed in  $^3\text{He-A}$  and can form different types of textures. The quasiparticles view the order parameter textures as the curved Lorentzian space-time and the gauge fields. These fields are dynamical: the effective Lagrangian for "electromagnetic" and "gravitational" fields can be obtained by integrating over the fermionic field. The same principle was used by Sakharov and Zeldovich to obtain the effective gravity [3] and the effective electrodynamics [4] from the vacuum fluctuations. In some

special cases (and in this review we consider just such a case) the main contribution to the effective action comes from the vacuum fermions which momenta  $\mathbf{p}$  are concentrated near the gap nodes, i.e. from the "relativistic" fermions. In these (and only in these) cases one obtains the effective Lagrangian, which gives the Maxwell equations for the  $\mathbf{A}$ -field. Since the "photons" are thus constructed from the fermionic degrees of freedom, the metric  $g^{ik}$ , which governs the propagation of "photons", is the same as the metric governing the dynamics of the underlying fermionic quasiparticles. This means that the "light" also propagates with the "speed of light". Following the title of the Laughlin talk at this Symposium this is an example of the Gauge Theory from Nothing [5].

From Eq.(3) it follows that  $g^{00} = -1$  and  $g^{0i} = 0$ , but this is not the general case: typically all the components of the dynamical metric tensor  $g_{\mu\nu}$  depend on space-time. In some cases the effective metric is not trivial giving rise to the conical singularities [6], event horizons and ergoregions [7,8]. This also allows to simulate the quantum gravity. Note that the primary quantities in this effective (quantum) gravity are the contravariant metric elements  $g^{\mu\nu}$ . They appear in the low-energy corner of the fermionic spectrum and represent the low-energy properties of quantum vacuum. The effective space-time, where the free quasiparticles follow a geodesic, is determined by the inverse metric  $g_{\mu\nu}$  and thus is the secondary object. In a similar manner the effective Lorentzian space-time comes from the spectrum of the sound waves propagating on the background of a moving inhomogeneous liquid [9–11]. The difference from the case of the superfluid liquid  $^3\text{He-A}$  is that ordinary liquids are essentially dissipative systems and cannot serve as a model of the quantum vacuum.

The above mechanism of the generation of the gauge field and gravity is valid for the general system with the point gap nodes. In the particular case of the  $^3\text{He-A}$  the initial "nonrelativistic" fermionic spectrum has the form

$$E^2(\mathbf{p}) = v_F^2(p - p_F)^2 + \frac{\Delta_A^2}{p_F^2}(\hat{\mathbf{I}} \times \mathbf{p})^2, \quad (5)$$

where  $\Delta_A$  is the gap amplitude;  $v_F = p_F/m^*$  is Fermi velocity;  $m^*$  is the effective mass of the quasiparticle in the normal Fermi-liquid state, which is typically about 3-6 of the bare mass  $m_3$  of the  $^3\text{He}$  atom.

In the low energy corner one obtains the "relativistic" spectrum in Eq.(3) with the following values of the "fundamental constants" [12,13]

$$c_1 = c_2 = \frac{\Delta_A}{p_F} \equiv c_\perp, \quad c_3 = v_F \equiv c_\parallel. \quad (6)$$

The space characterizing the motion of quasiparticles in  $^3\text{He-A}$ , i.e. the space in which the quasiparticles move along the geodesic curves (in the absence of other forces) has an uniaxial anisotropy with anisotropy axis along  $\hat{\mathbf{I}}$ :

$$\hat{\mathbf{e}}_3 = \hat{\mathbf{I}}. \quad (7)$$

The "speed of light" propagating along  $\hat{\mathbf{I}}$ -vector,  $c_\parallel$ , is about 3 orders of magnitude larger than that in the transverse direction:  $c_\parallel \gg c_\perp$ . Another important fundamental constant,  $\Delta_A$ , plays the role of the Planck energy, as will be illustrated later on.

## B. Chiral fermions in $^3\text{He-A}$

The chiral properties of the fermionic spectrum can be revealed after the square root of Eq.(3) is taken. This procedure is not unambiguous, so one must use the underlying BCS theory of the Cooper pairing which leads to the superfluid A-phase state in  $^3\text{He}$ . In the BCS theory one obtains the Bogoliubov-Nambu Hamiltonian for the fermions, which in the low-energy corner transforms to the Weyl Hamiltonian for massless chiral particles. It represents the proper square root of Eq.(3):

$$\mathcal{H} = -e \sum_a c_a \tau^a \hat{e}_a^i (p_i - eA_i), \quad (8)$$

where  $\tau^a$  are the Pauli matrices acting in the Bogoliubov-Nambu particle-hole space.

The important property of this Hamiltonian is that the sign of the "electric" charge  $e$  simultaneously determines the chirality of the fermions. This is clearly seen on a simple isotropic example with  $c_1 = c_2 = c_3 = c$ :

$$\mathcal{H} = -ec\vec{\tau} \cdot (\mathbf{p} - e\mathbf{A}). \quad (9)$$

Particle with positive (negative)  $e$  is left-handed (right-handed): its Bogoliubov spin  $\vec{\tau}$  is antiparallel (parallel) to the momentum  $\mathbf{p}$ . Thus the field  $\mathbf{A}$  corresponds to the axial field in relativistic theories. The symmetry between left and right is broken in  $^3\text{He-A}$ .

Existence of the chiral particles in the 3+1 space-time is the unique property of superfluid  $^3\text{He-A}$  and also of the Standard model of the electroweak interactions. That is why  $^3\text{He-A}$  is the best condensed matter for the simulations of effects related to the chiral nature of the fermions, especially of the effect of chiral anomaly. There are some other condensed matter systems with the chiral fermions, but these fermions live in the 2+1 or 1+1 dimensions. Examples are the 2+1 fermions in high-temperature superconductors [14]; 1+1 chiral edge states in the Quantum Hall Effect [15,16] and in the superconductors with broken time-reversal symmetry [17,18], and also the fermionic excitations in the core of quantized vortices [8]. The gap nodes in 3+1 theories can appear also in different types of "color superfluidity" – quark condensates in a dense barionic matter [19].

The spectrum of fermionic excitations of the electroweak vacuum contains the branch of the chiral particles: left-handed neutrino (Fig. 2). The right-handed

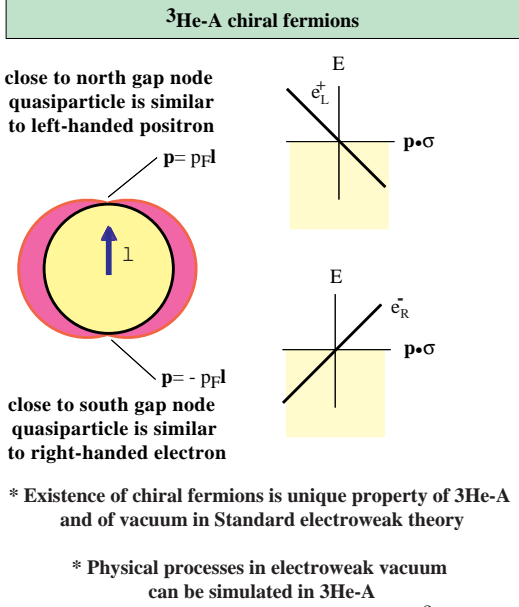


FIG. 1. Gap nodes and chiral fermions in  ${}^3\text{He-A}$ . Close to the gap nodes the gapless quasiparticle represent the massless fermions moving in the electromagnetic and gravity fields and obeying the relativistic equation. The lefthanded particles have positive charge  $e = +1$  and are in the vicinity of the north pole determined by the direction of the  $\hat{l}$ -vector, while the right particles with  $e = -1$  are in the vicinity of the south pole. If the  $\hat{l}$ -field is not uniform in space and time the space and time derivative of  $\mathbf{A} = p_F \hat{l}$  act on the quasiparticle as magnetic and electric field correspondingly.

neutrino is absent (or interacts with the other matter differently than the left-handed one). This is the remarkable manifestation of the violation of the left-right symmetry in the electroweak vacuum. Another symmetry, which is broken in the present Universe, is the  $SU(2)$  symmetry of weak interactions. In the unbroken symmetry state of the early Universe, the left leptons (neutrino and left electron) form the  $SU(2)$  doublet, while the right electron is the  $SU(2)$  singlet. During the cool down of the Universe the phase transition (or the crossover) occurred, at which the  $SU(2) \times U(1)$  symmetry was broken. As a result the left and right electrons were hybridized forming the present electronic spectrum with the gap  $\Delta = m_e c^2$ . The electric properties of the vacuum thus exhibited the metal-insulator transition: The "metallic" state of the vacuum with the Fermi point in the electronic spectrum was transformed to the insulating state with the gap.

The similarity between the chiral fermions in electroweak theory and in  ${}^3\text{He-A}$  has also the topological origin. The gap nodes – zeroes in the particle (quasiparticle) spectrum – are characterized by the  $\pi_3$  topological invariant in the 4-momentum space [12]:

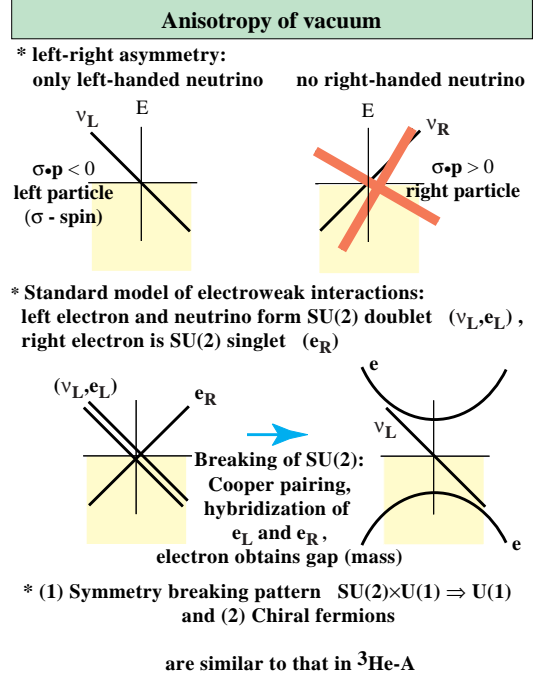


FIG. 2. (*top*): The spectrum of fermionic excitations of the physical vacuum contain the branch of the chiral particles: left-handed neutrino. The right-handed neutrino is absent. In the unbroken symmetry state of the early Universe, the left leptons (neutrino and left electron) formed the  $SU(2)$  doublet, while the right electron was the  $SU(2)$  singlet. (*bottom*): During the cool down of the Universe the phase transition (or the crossover) occurred, at which the  $SU(2)$  symmetry was broken. As a result the left and right electrons were hybridized forming the present electronic spectrum with the gap  $\Delta = m_e c^2$ . The electric properties of the vacuum thus exhibited the metal-insulator transition.

$$N_{\text{top}} = \frac{1}{24\pi^2} e_{\mu\nu\lambda\gamma} \text{tr} \int_{\sigma} dS^{\gamma} \mathcal{G} \partial_{p^{\mu}} \mathcal{G}^{-1} \mathcal{G} \partial_{p^{\nu}} \mathcal{G}^{-1} \mathcal{G} \partial_{p^{\lambda}} \mathcal{G}^{-1}. \quad (10)$$

Here

$$\mathcal{G}(p_{\mu}) = \frac{1}{ip_0 + \mathcal{H}} \quad (11)$$

is the Green's function.  $\sigma$  is the 3D surface around the point node in the 4-momentum space. For the relativistic chiral particle the node is at  $p_0 = 0$ ,  $\mathbf{p} = 0$ , while in  ${}^3\text{He-A}$  the nodes are at  $p_0 = 0$ ,  $\mathbf{p} = \pm p_F \hat{l}$ . In all cases the topological invariant is nonzero:  $N_{\text{top}} = \pm 1$ , the sign of  $N_{\text{top}}$  depends on chirality.

## II. AXIAL ANOMALY

## A. ABJ equation.

The fermionic system with the chiral fermions exhibits effect of the chiral anomaly, the nonconservation of charge of the matter due to interaction with the quantum vacuum. The principle of the axial anomaly can be seen from the behavior of the chiral particle in a constant magnetic field,  $\mathbf{A} = (1/2)\mathbf{B} \times \mathbf{r}$ . The Hamiltonians for the right particle with the electric charge  $e_R$  and for the left particle with the electric charge  $e_L$  are

$$\mathcal{H} = c\vec{\tau} \cdot (\mathbf{p} - e_R\mathbf{A}), \mathcal{H} = -c\vec{\tau} \cdot (\mathbf{p} - e_L\mathbf{A}). \quad (12)$$

Fig. 3 shows the energy spectrum in a magnetic field  $\mathbf{B}$  along  $z$ ; the thick lines show the occupied negative-energy states. Motion of the particles in the plane perpendicular to  $\mathbf{B}$  is quantized into the Landau levels shown. The free motion is thus effectively reduced to one-dimensional motion along  $\mathbf{B}$  with momentum  $p_z$ . Because of the chirality of the particles the lowest ( $n = 0$ ) Landau level is asymmetric. It crosses zero only in one direction:  $E = cp_z$  for right particle and  $E = -cp_z$  for the left one. If we now apply an electric field  $\mathbf{E}$  along  $z$ , particles are pushed from negative to positive energy levels according to the equation of motion  $\dot{p}_z = e_R E$  ( $\dot{p}_z = e_L E$ ) and the whole Dirac sea moves up (down) creating particles and electric charge from the vacuum. This motion of the particles along the ‘‘anomalous’’ branch of the spectrum is called spectral flow. The rate of particle production is proportional to the density of states at the Landau level, which is  $\propto |e_R\mathbf{B}|$  ( $|e_L\mathbf{B}|$ ), so that the rate of production of particle number  $n$  and of charge  $Q = n(e_R + e_L)$  from the vacuum is

$$\dot{n} = \frac{1}{4\pi^2}(e_R^2 - e_L^2)\mathbf{E} \cdot \mathbf{B}, \quad \dot{Q} = \frac{1}{4\pi^2}(e_R^3 - e_L^3)\mathbf{E} \cdot \mathbf{B} \quad (13)$$

This is an anomaly equation for the production of particles from the vacuum of the type found by Adler [20] and by Bell and Jackiw [21] in the context of neutral pion decay. We see that for particle or charge creation from ‘‘nothing’’ it is necessary to have an asymmetric branch of the dispersion relation  $E(p)$  which crosses the axis from negative to positive energy, and also the symmetry between the left and right particles should be violated:  $e_R \neq e_L$ .

## B. Anomalous nucleation of the baryonic charge

In the Standard electroweak model there is an additional accidental global symmetry  $U(1)_B$  whose classically conserved charge is the baryon number  $Q_B$ . Each of the quarks is assigned  $Q_B = 1/3$  while the leptons (neutrino and electron) have  $Q_B = 0$ . This baryonic number is not conserved due to the axial anomaly. There are two gauge fields which ‘‘electric’’ and ‘‘magnetic’’ fields

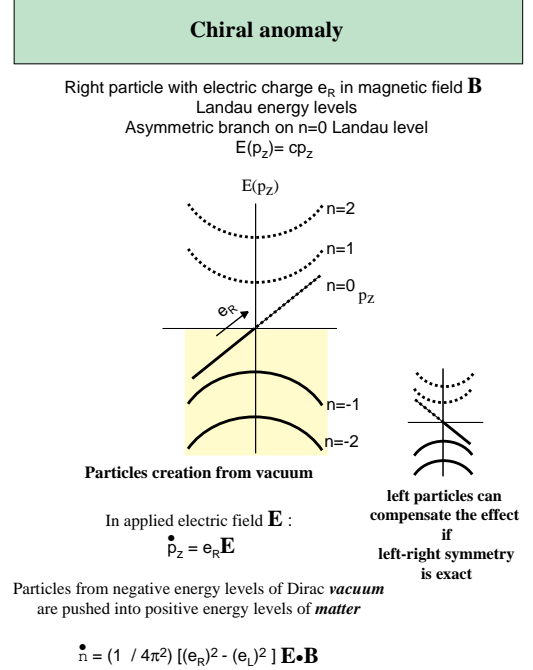


FIG. 3. Chiral anomaly: the spectral flow from the occupied energy levels caused by the applied electric field leads to the creation of the fermionic charge from the vacuum if the left-right symmetry is violated.

become source for the baryproduction: the hypercharge field  $U(1)$  and the weak field  $SU(2)$ . The corresponding hypercharges  $Y$  and weak charges  $W$  of the left  $u$  and  $d$  quarks are

$$Y_{dL} = Y_{uL} = 1/6, \quad W_{dL} = -W_{uL} = 1/2, \quad (14)$$

while for the right  $u$  and  $d$  quarks one has

$$Y_{uR} = 2/3, \quad Y_{dR} = -1/3, \quad W_{dR} = W_{uR} = 0. \quad (15)$$

Let us first consider the effect of the hypercharge field. Since the number of different species of quarks carrying the baryonic charge is  $3N_F$  (3 colours  $\times N_F$  generations of fermions) and the baryonic charge of quark is  $Q_B = 1/3$ , the production rate of the baryonic charge in the presence of hyperelectric and hypermagnetic fields is

$$\frac{N_F}{4\pi^2} (Y_{dR}^2 + Y_{uR}^2 - Y_{dL}^2 - Y_{uL}^2) \mathbf{B}_Y \cdot \mathbf{E}_Y \quad (16)$$

Since the hypercharges of left and right quarks are different (see Eqs.(14,15)) one obtains the nonzero production of baryons by the hypercharge field

$$\frac{N_F}{8\pi^2} \mathbf{B}_Y \cdot \mathbf{E}_Y \quad (17)$$

The weak electric and magnetic fields also contribute to the production of the baryonic charge:

$$\frac{N_F}{4\pi^2}(W_{dR}^2 + W_{uR}^2 - W_{dL}^2 - W_{uL}^2) \mathbf{B}_W^a \cdot \mathbf{E}_{aW} , \quad (18)$$

which gives

$$- \frac{N_F}{8\pi^2} \mathbf{B}_W^a \cdot \mathbf{E}_{aW} \quad (19)$$

Thus the total rate of baryon production in the Standard model is

$$\dot{Q}_B = \frac{N_F}{8\pi^2} (-\mathbf{B}_W^a \cdot \mathbf{E}_{aW} + \mathbf{B}_Y \cdot \mathbf{E}_Y) \quad (20)$$

### C. Anomalous nucleation of linear momentum in ${}^3\text{He-A}$ .

The anomaly equation which describes the nucleation of the fermionic charges in the presence of magnetic and electric fields describes both the production of the baryons in the electroweak vacuum (baryogenesis) and the production of the linear momentum in the superfluid  ${}^3\text{He-A}$  (momentogenesis). In  ${}^3\text{He-A}$  the effective  $U(1)$  gauge field is generated by the moving texture. According to Eq.(2), the time and space dependent  $\hat{\mathbf{l}}$  vector associated with the motion of the vortex produces a force on the excitations equivalent to that of an “electric” (or “hyperclectric”) field  $\mathbf{E} = p_F \partial_t \hat{\mathbf{l}}$  and a “magnetic” (or “hypermagnetic” field)  $\mathbf{B} = p_F \nabla \times \hat{\mathbf{l}}$  acting on particles of unit charge. Equation (13) can then be applied to calculate the rate at which left-handed and right-handed quasiparticles are created by spectral flow. What we are interested in is the production of the particle momentum due to spectral flow:

$$\dot{\mathbf{P}} = \frac{1}{4\pi^2} (\mathbf{P}_R - \mathbf{P}_L) (\mathbf{E} \cdot \mathbf{B}) . \quad (21)$$

Since the right and left particle have opposite momenta  $\mathbf{P}_R = p_F \hat{\mathbf{l}} = -\mathbf{P}_L$ , excitation momentum is created at a rate

$$\dot{\mathbf{P}} = \frac{p_F^3}{2\pi^2} \hat{\mathbf{l}} (\partial_t \hat{\mathbf{l}} \cdot (\vec{\nabla} \times \hat{\mathbf{l}})) . \quad (22)$$

However, total linear momentum of the liquid must be conserved. Therefore Eq. (22) means that, in the presence of a time-dependent texture, momentum is transferred from the superfluid ground state (analogue of vacuum) to the heat bath of excitations forming the normal component (analogue of matter).

## III. SPECTRAL FLOW FORCE ON VORTEX

### A. Continuous vortex and baryogenesis in textures.

The anomalous production of the linear momentum leads to the additional force acting on the continuous vortex in  ${}^3\text{He-A}$  (Fig. 4).

The continuous vortex, first discussed by Chechetkin [22] and Anderson and Toulouse [23] (ATC vortex), in its simplest realization has the following distribution of the  $\hat{\mathbf{l}}$ -field ( $\hat{\mathbf{z}}$ ,  $\hat{\mathbf{r}}$  and  $\hat{\phi}$  are unit vectors of the cylindrical coordinate system)

$$\hat{\mathbf{l}}(r, \phi) = \hat{\mathbf{z}} \cos \eta(r) + \hat{\mathbf{r}} \sin \eta(r) , \quad (23)$$

where  $\eta(r)$  changes from  $\eta(0) = \pi$  to  $\eta(\infty) = 0$  in the so called soft core of the vortex. The superfluid velocity  $\mathbf{v}_s$  in superfluid  ${}^3\text{He-A}$  is determined by the twist of the triad  $\hat{\mathbf{e}}_1, \hat{\mathbf{e}}_2, \hat{\mathbf{e}}_3$  and corresponds to the torsion in the tetrad formalism of the gravity:

$$\mathbf{v}_s = \frac{\hbar}{2m_3} \hat{\mathbf{e}}_1^i \vec{\nabla} \hat{\mathbf{e}}_2^i . \quad (24)$$

As distinct from other (singular) vortices, in the continuous vortex the superfluid velocity field

$$\mathbf{v}_s(r, \phi) = -\frac{\hbar}{2m_3 r} [1 + \cos \eta(r)] \hat{\phi} , \quad (25)$$

has no singularity on the vortex axis.

The stationary vortex generates the “magnetic” field and when the vortex moves with a constant velocity  $\mathbf{v}_L$  it also generates the “electric” field, since  $\hat{\mathbf{l}}$  depends on  $\mathbf{r} - \mathbf{v}_L t$ :

$$\mathbf{B} = p_F \vec{\nabla} \times \hat{\mathbf{l}} , \quad \mathbf{E} = \partial_t \mathbf{A} = -p_F (\mathbf{v}_L \cdot \vec{\nabla}) \hat{\mathbf{l}} \quad (26)$$

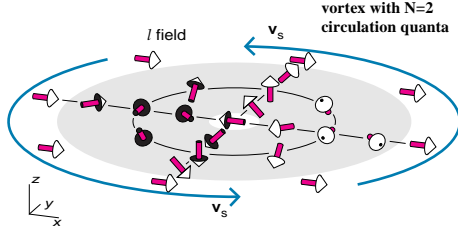
The net production of the quasiparticle momenta by the spectral flow in the moving vortex means that, when the vortex moves with respect to the system of quasiparticles (the normal component of liquid or matter, which flow is characterised by the normal velocity  $\mathbf{v}_n$ ), there is force acting between the normal component and the vortex. Integration of the anomalous momentum transfer in Eq.(22) over the cross-section of the soft core of the moving ATC vortex gives the following force acting on the vortex (per unit length) from the system of quasiparticles [24]:

$$\mathbf{F}_{sf} = \int d^2 r \frac{p_F^3}{2\pi^2} \hat{\mathbf{l}} (\partial_t \hat{\mathbf{l}} \cdot (\vec{\nabla} \times \hat{\mathbf{l}})) = -2\pi \hbar C_0 \hat{\mathbf{z}} \times (\mathbf{v}_L - \mathbf{v}_n), \quad (27)$$

where

$$C_0 = p_F^3 / 3\pi^2 . \quad (28)$$

### Momentogenesis by continuous ATC vortex



Momentum transfer from the vacuum (superfluid) to the heat bath (matter) gives extra force on N=2 vortex

$$\begin{aligned} \mathbf{F} &= \int d^3r \dot{\hat{\mathbf{l}}} = (1/2\pi^2) \int d^3r (\mathbf{B} \cdot \mathbf{E}) p_F \mathbf{l} \\ &= (1/2\pi^2) \hbar p_F^3 \int d^3r (\nabla \times \mathbf{l} \cdot d\mathbf{l}/dt) \mathbf{l} \\ &= \pi \hbar N (1/3\pi^2) p_F^3 \hat{\mathbf{z}} \times (\mathbf{v}_n - \mathbf{v}_L) \end{aligned}$$

This force effectively cancels the Magnus force

$$\mathbf{F}_M = \pi \hbar N n_3 \mathbf{z} \times (\mathbf{v}_s - \mathbf{v}_L).$$

The density of  $^3\text{He}$  atoms  $n_3$  deviates from  $(1/3\pi^2) p_F^3$  due to small asymmetry between particles and holes

FIG. 4. The order parameter  $\hat{\mathbf{l}}$ -texture (analog of the vector potential of (hyper) electromagnetic field) in the soft core of continuous Anderson-Toulouse-Chechetkin vortex [22,23] (ATC vortex). The moving vortex converts the textural (vacuum) fermionic charge (linear momentum) to the system of the fermionic quasiparticles (matter). The moving vortex generates the time dependence of the order parameter, which is equivalent to electric field  $\mathbf{E}$ . Together with the effective magnetic field  $\mathbf{B}$  concentrated in the soft core of ATC vortex this gives rise to  $\mathbf{B} \cdot \mathbf{E}$  which is the anomalous source of the fermionic charge.

Note that this spectral-flow force is transverse to the relative motion of the vortex and thus is nondissipative (reversible). In this derivation it was assumed that the quasiparticles and their momenta, created by the spectral flow from the vacuum, are finally absorbed by the normal component. The time delay of this process and the viscosity lead to the dissipative (friction) force between the vortex and the normal component:  $\mathbf{F}_{fr} = -\gamma(\mathbf{v}_L - \mathbf{v}_n)$ . There is no momentum exchange between the vortex and the normal component if they move with the same velocity.

Another important property of the spectral-flow force that it does not depend on the details of the vortex structure: the result for  $\mathbf{F}_{sf}$  is robust to any deformation of the  $\hat{\mathbf{l}}$ -texture which does not change the asymptote, i.e. the topology of the vortex. In this respect this force reminds another force, acting on the vortex from the superfluid (vacuum) motion. This is the well-known Magnus force:

$$\mathbf{F}_M = 2\pi \hbar n_3 \hat{\mathbf{z}} \times (\mathbf{v}_L - \mathbf{v}_s(\infty)). \quad (29)$$

Here  $n_3$  is the particle density (here the number density of  $^3\text{He}$  atoms) and  $\mathbf{v}_s(\infty)$  is the uniform velocity of the superfluid vacuum far from the vortex.

The balance between all the forces acting on the vortex,  $\mathbf{F}_{sf}$ ,  $\mathbf{F}_{fr}$ ,  $\mathbf{F}_M$  and some other forces including the external force and the so-called Iordanskii force coming from the Aharonov-Bohm effect, determines the velocity of the vortex  $\mathbf{v}_L$  as linear combination of  $\mathbf{v}_s(\infty)$  and  $\mathbf{v}_n$ .

The result for the spectral-flow force, derived for the ATC vortex from the axial anomaly equation (22), was confirmed in the microscopic theory, which took into account the discreteness of the quasiparticle spectrum in the soft core [25]. This was also confirmed in experiments on vortex dynamics in  $^3\text{He-A}$  [26,27].

In this experiment a uniform array of vortices is produced by rotating the whole cryostat. In equilibrium the vortices and the normal component of the fluid (heat bath) rotate together with the cryostat. The electrostatically driven vibrating diaphragm produces oscillating superflow, which via the Magnus force generates the vortex motion, while the normal component remains clamped by its high viscosity. This creates the motion of vortices with respect both to the heat bath and superfluid vacuum. The vortex velocity  $\mathbf{v}_L$  is determined by the overall balance of forces acting on the vortices: [26]

$$\hat{\mathbf{z}} \times (\mathbf{v}_L - \mathbf{v}_s(\infty)) + d_{\perp} \hat{\mathbf{z}} \times (\mathbf{v}_n - \mathbf{v}_L) + d_{\parallel} (\mathbf{v}_n - \mathbf{v}_L) = 0. \quad (30)$$

Measurement of the damping of the diaphragm resonance and of the coupling between different eigen modes of vibrations enables both  $d_{\perp}$  and  $d_{\parallel}$  to be deduced.

From the above theory of the spectral flow in the  $^3\text{He-A}$  vortex texture it follows that the parameter

$$d_{\perp} \approx \frac{C_0 - n_3 + n_s(T)}{n_s(T)} \quad (31)$$

where  $n_s(T)$  is the density of the superfluid component. In this equation the parameter  $C_0$  in Eq.(28) comes from the axial anomaly, the particle density  $n_3$  – from the Magnus force and the superfluid density  $n_s(T)$  – from the combined effect of the Magnus and Iordanskii forces. The effect of the chiral anomaly is crucial for the parameter  $d_{\perp}$  since  $C_0$  is comparable with  $n_3$ . Moreover it appears that  $C_0$  is very close to  $n_3$ , since  $C_0 = p_F^3/3\pi^2$  is the particle density of the liquid  $^3\text{He}$  in the absence of superfluidity. The difference between  $C_0$  and  $n_3$  is thus determined by the tiny effect of the superfluidity on the particle density and is extremely small:  $n_3 - C_0 \sim n_3(\Delta_A/v_F p_F)^2 = n_3(c_{\perp}/c_{\parallel})^2 \ll n_3$ . So due to the axial anomaly one must have  $d_{\perp} \approx 1$  for all practical temperatures, even including the region close to  $T_c$ , where the superfluid component  $n_s(T) \sim n_3(1 - T^2/T_c^2)$  is small. The  $^3\text{He-A}$  experiments, made in the whole temperature range, where the  $^3\text{He-A}$  is stable, gave precisely this value within experimental uncertainty,  $|1 - d_{\perp}| < 0.005$  [26].

This produces an experimental verification of the Adler-Bell-Jackiw axial anomaly equation (13) applied to  ${}^3\text{He-A}$  and thus supports the idea that the baryonic charge (and also the leptonic charge) can be generated by the electroweak fields.

### B. Singular vortex and baryogenesis by cosmic strings.

There are many different scenarios of the electroweak baryogenesis [28,29]. In some of them the baryonic charge can be created in the cores of the topological objects, in particular in the core of cosmic strings. While a weak and hypercharge magnetic flux is always present in the core of electroweak strings, a weak and hypercharge electric field can also be present along the string if the string is moving across a background electromagnetic field [30] or in certain other processes such as the de-linking of two linked loops [31,32]. Parallel electric and magnetic fields in the string change the baryonic charge and can lead to cosmological baryogenesis [33] and to the presence of antimatter in cosmic rays [34].

Again the axial anomaly is instrumental for the baryoproduction in the core of cosmic strings. But now the effect cannot be described by the anomaly equation (13). This equation was derived using the energy spectrum of the free massless fermions in the presence of the homogeneous electric and magnetic fields. But in cosmic strings these fields are no more homogeneous. Moreover the massless fermions exist only in the vortex core as bound states in the potential well produced by the order parameter (Higgs) field. So the consideration of the baryoproduction should be essentially different: the spectral flow phenomenon should be studied using an exact spectrum of the massless bound states, fermion zero modes on strings.

Similar situation takes place in condensed matter, where the counterpart of the cosmic string is the quantized vortex with a singular core (Fig.5). As in the case of continuous ATC vortex, the momentogenesis due to axial anomaly takes place. But for its description one should consider the spectral properties of the fermion zero modes localized in the vortex core. The main difference between the fermion zero modes in the relativistic strings and in the conventional condensed matter vortices is the following. In the strings the anomalous branch  $E(p_z)$  which crosses zero and gives rise to the spectral flow from the negative energy levels of the vacuum to the positive energy levels of the matter is in terms of continuous variable – the linear momentum  $p_z$  along the string. In the quantized vortices (Fig. 6) this is the branch of  $E(L_z)$ , which "crosses" zero as a function of the discrete angular momentum  $\hbar L_z$  ( $L_z$  can be integral or half-odd integral). The level flow along the discrete energy levels is suppressed and is determined by the interlevel distance

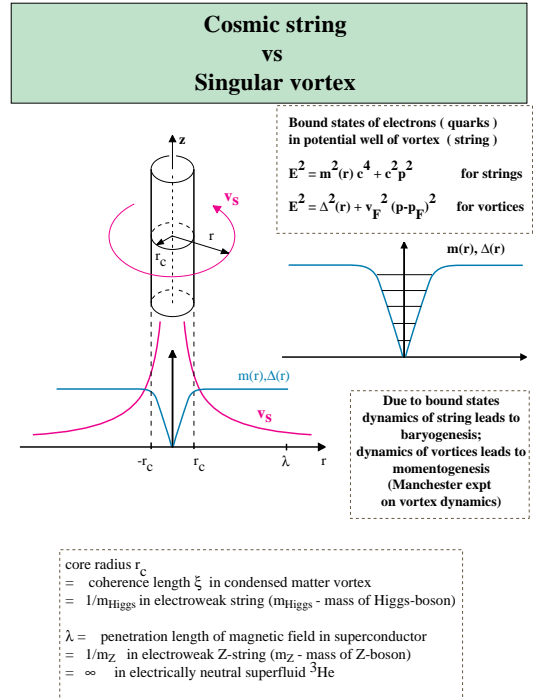


FIG. 5. Cosmic string is the counterpart of the Abrikosov vortex in superconductor. It also contains the bound states of the fermions, which are important for the baryoproduction.

$\hbar\omega_0$  and the level width  $\hbar/\tau$  resulting from the scattering of core excitations by free excitations in the heat bath outside the core (or by impurities in superconductors).

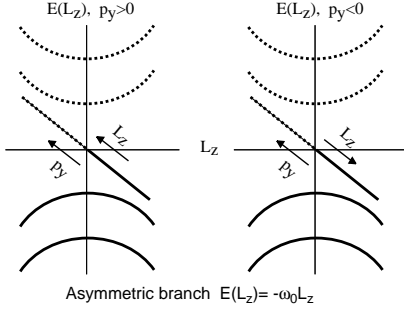
This suppression of the spectral flow results in the renormalization of the spectral-flow parameter, which is roughly

$$\tilde{C}_0 \sim \frac{C_0}{1 + \omega_0^2 \tau^2} \quad (32)$$

$$d_{\perp} \approx \frac{\tilde{C}_0 - n_3 + n_s(T)}{n_s(T)} \quad (33)$$

If  $\omega_0\tau \ll 1$  the levels overlap and the spectral flow is allowed. In the opposite limit  $\omega_0\tau \gg 1$  it is completely suppressed. The parameter  $\omega_0\tau$  depends on temperature and this allows us to check the Eq.(33) experimentally. This has been done in Manchester experiment on dynamics of singular vortices in  ${}^3\text{He-B}$  [26,27]: The equation of the type of (33) has been verified in the broad temperature range, which included both extreme limits,  $\omega_0\tau \ll 1$  and  $\omega_0\tau \gg 1$ .

**Anomalous nonconservation of linear momentum  
in superconductors and in  $^3\text{He-B}$  vortex**



When vortex moves along  $x$  the angular momentum changes

$$\dot{L}_z = \dot{x} p_y = v_x p_y$$

This gives the flow of levels from Fermi sea

$$\dot{n} = \dot{L}_z / \hbar = v_x p_y / \hbar$$

The flow of linear momentum (transverse force on vortex)

$$F_y = \langle \dot{p}_y \rangle = \langle p_y \dot{n} \rangle = \langle p_y^2 \rangle v_x / \hbar = \pi \hbar (1/3\pi^2) p_F^3 v_x$$

FIG. 6. The spectral flow of the momentum in the core of the moving singular vortex leads to the experimentally observed reactive force on a vortex in superfluid  $^3\text{He-B}$ .

#### IV. MAGNETIC FIELD FROM FERMIONIC CHARGE

Recent scenario of generation of the primordial magnetic field by Joyce and Shaposhnikov [35,36] is based on the effect, which is opposite to that discussed in previous Section: the axial anomaly gives rise to transformation of the excess of chiral particles into the hypermagnetic field. In the  $^3\text{He-A}$  language this process describes the collapse of the excitation momenta (fermionic charge) towards the formation of the textures – counterpart of the hypermagnetic field in the Joyce-Shaposhnikov scenario [38] (Figs. 7,8). Such collapse was recently observed in Helsinki rotating cryostat [37,38].

##### A. Effective Lagrangian at low $T$ .

To study the instability of the superflow and to relate it to the problem of the magnetogenesis, let us start with the relevant effective Lagrangian for the superfluid dynamics at low  $T$  and find the correspondence to the effective Lagrangian for the system of chiral fermions interacting with the magnetic or hypermagnetic field via axial anomaly.

Let us consider the superfluid moving with respect to the vessel walls. The normal component of the liquid is clamped by the vessel walls due to its high viscosity, so

the normal velocity  $\mathbf{v}_n = 0$  in the reference frame moving with the vessel. If the superfluid velocity  $\mathbf{v}_s$  of the condensate in Eq.(24) is nonzero in the vessel frame, one has a nonzero counterflow of superfluid and normal component with the relative velocity  $\mathbf{w} = \mathbf{v}_s - \mathbf{v}_n$ . This relative velocity provides the nonzero fermionic charge, as will be seen below, and the flow instability leads to transformation of this charge to the analog of the hypermagnetic field. Let us choose the axis  $z$  along the velocity  $\mathbf{w}$  of the counterflow. In equilibrium the unit orbital vector  $\hat{\mathbf{l}}$  is oriented along the counterflow:  $\hat{\mathbf{l}}_0 = \hat{\mathbf{z}}$ . The stability problem is investigated using the quadratic form of the deviations of the superfluid velocity and  $\hat{\mathbf{l}}$ -vector from their equilibrium values:

$$\hat{\mathbf{l}} = \hat{\mathbf{l}}_0 + \delta\hat{\mathbf{l}}(\mathbf{r}, t) - \frac{1}{2}\hat{\mathbf{l}}_0(\delta\hat{\mathbf{l}}(\mathbf{r}, t))^2, \quad \mathbf{v}_s = \mathbf{w}_0 + \delta\mathbf{v}_s(\mathbf{r}, t). \quad (34)$$

The instability of the counterflow towards generation of the inhomogeneity  $\delta\hat{\mathbf{l}}(\mathbf{r}, t)$ , corresponds to the generation of magnetic field  $\mathbf{B} = p_F \nabla \times \delta\hat{\mathbf{l}}$  from the chiral fermions.

The energy of the liquid in terms of  $\hat{\mathbf{l}}$  and  $\mathbf{v}_s$  is [39]

$$F = \frac{1}{2} m_3 n_s^{ij} v_{si} v_{sj} + C_0 (\mathbf{v}_s \cdot \hat{\mathbf{l}}) (\hat{\mathbf{l}} \cdot (\nabla \times \hat{\mathbf{l}})) + K_b (\hat{\mathbf{l}} \times (\nabla \times \hat{\mathbf{l}}))^2 \quad (35)$$

(1) The first term in Eq.(35) is the kinetic energy of superflow with  $n_s^{ij}$  being an anisotropic tensor of superfluid density. At low  $T$  one has

$$n_s^{ij} \approx n_3 \delta^{ij} - n_{n\parallel} \hat{l}^i \hat{l}^j, \quad n_{n\parallel} \approx \frac{m^*}{3m_3} p_F^3 \frac{T^2}{\Delta_0^2}. \quad (36)$$

(2) The second term in Eq.(35) is the anomalous interaction of the superflow with  $\hat{\mathbf{l}}$ -texture, which comes from the axial anomaly [12]. The anomaly parameter  $C_0$  at  $T = 0$  is the same as in Eq.(28).

(3) Finally the third term is the relevant energy of  $\hat{\mathbf{l}}$ -texture. There are two other terms in the textural energy [39], containing  $(\hat{\mathbf{l}} \cdot (\nabla \times \hat{\mathbf{l}}))^2$  and  $(\nabla \cdot \hat{\mathbf{l}})^2$ , but they are not important for the stability problem: The instability starts with growing the  $z$ -dependent disturbances, so we are interested only  $z$ -dependent  $\hat{\mathbf{l}}$ -texture which in quadratic approximation contributes only the term  $(\hat{\mathbf{l}} \times (\nabla \times \hat{\mathbf{l}}))^2$ . The rigidity  $K_b$  at low  $T$  is logarithmically divergent

$$K_b = \frac{p_F^2 v_F}{24\pi^2 \hbar} \ln \left( \frac{\Delta_0^2}{T^2} \right). \quad (37)$$

There is also the topological connection between  $\hat{\mathbf{l}}$  and  $\mathbf{v}_s$ , since  $\mathbf{v}_s$  in Eq.(24) is the torsion of the dreibein field. This leads to the nonlinear connection, the so-called Mermin-Ho relation, which in our geometry gives

$$\delta \mathbf{v}_s = \frac{\hbar}{2m_3} \hat{\mathbf{z}} \partial_z \phi + \frac{\hbar}{4m_3} \delta \hat{\mathbf{l}} \times \partial_z \delta \hat{\mathbf{l}} \quad (38)$$

The three variables, the potential  $\phi$  of the flow velocity and two components  $\delta \hat{\mathbf{l}} \perp \hat{\mathbf{l}}_0$  of the unit vector  $\hat{\mathbf{l}}$ , is just another presentation of 3 rotational degrees of freedom of the dreibein  $\hat{\mathbf{e}}_1, \hat{\mathbf{e}}_2, \hat{\mathbf{e}}_3$ . While  $\delta \hat{\mathbf{l}}$  is responsible for the effective vector potential of the (hyper) magnetic field, the variable  $\phi$  represents the axion field as we shall see later.

Let us expand the energy in terms of the small perturbations. Adding the terms with time derivatives we obtain the following Lagrangian for  $\phi$  and  $\delta \hat{\mathbf{l}}$ :

$$L = F_0 + L_{\delta \hat{\mathbf{l}}} + L_\phi. \quad (39)$$

Here  $F_0$  is the initial homogeneous flow energy

$$F_0 = \frac{1}{2} m_3 n_3 \mathbf{w}_0^2 - \frac{m^*}{6m_3} p_F^3 \frac{T^2}{\Delta_0^2} (\mathbf{w}_0 \cdot \hat{\mathbf{l}}_0)^2 \quad (40)$$

$L_{\delta \hat{\mathbf{l}}}$  is the textural Lagrangian:

$$L_{\delta \hat{\mathbf{l}}} = \frac{p_F^2}{24\pi^2 \hbar v_F} \ln \left( \frac{\Delta_0^2}{T^2} \right) \left[ v_F^2 (\partial_z \delta \hat{\mathbf{l}})^2 - (\partial_t \delta \hat{\mathbf{l}})^2 \right] \quad (41)$$

$$+ \frac{p_F^3}{2\pi^2} (\hat{\mathbf{l}}_0 \cdot \mathbf{w}_0) (\delta \hat{\mathbf{l}} \cdot \nabla \times \delta \hat{\mathbf{l}}) \quad (42)$$

$$+ \frac{m^*}{6} p_F^3 \frac{T^2}{\Delta_0^2} (\mathbf{w}_0 \cdot \hat{\mathbf{l}}_0)^2 (\delta \hat{\mathbf{l}})^2 \quad (43)$$

The first term describes the propagation of the textural waves (the so-called orbital waves).

The other terms will be discussed later. Here we only note that the term in Eq.(42) is the consequence of the axial anomaly, and there are 3 contributions to the factor  $\frac{p_F^3}{2\pi^2}$  in Eq.(42): (i) The factor  $C_0$  comes from Eq.(35). (ii) The factor  $n_3/2$  – from Eq.(38). And (iii) the factor  $-(n_3 - C_0)/2$  – from the intrinsic angular momentum, which gives the following contribution to the action [12]

$$\frac{1}{2} (n_3 - C_0) \left( \hat{\mathbf{l}}_0 \cdot (\delta \hat{\mathbf{l}} \times (\partial_t \delta \hat{\mathbf{l}} + (\mathbf{w} \cdot \nabla) \delta \hat{\mathbf{l}}) \right). \quad (44)$$

We do not discuss the problem of the intrinsic angular momentum here, though it is also related to the axial anomaly and spectral flow [40]. Altogether they give  $C_0 + n_3/2 - (n_3 - C_0)/2 = (3/2)C_0 = p_F^3/2\pi^2$  in Eq.(42).

$L_\phi$  is the variation of the Lagrangian for superflow. At low  $T$  one has

$$L_\phi = \frac{\hbar^2}{8m_3} n_3 \left[ (\partial_z \phi)^2 - \frac{1}{s^2} (\partial_t \phi)^2 \right] \quad (45)$$

$$+ \frac{3\hbar}{4m_3} C_0 \partial_z \phi (\delta \hat{\mathbf{l}} \cdot \nabla \times \delta \hat{\mathbf{l}}) \quad (46)$$

The first two terms of this Lagrangian, the Eq.(45), describe the propagation of sound waves (phonons), and  $s$  is a speed of sound. We shall later relate the sound waves to axions according to the third term in Lagrangian  $L_\phi$ , the Eq.(46), which contains the anomaly parameter  $C_0$ .

Let us establish all this correspondence.

### Counterflow vs chemical potential for chiral fermions

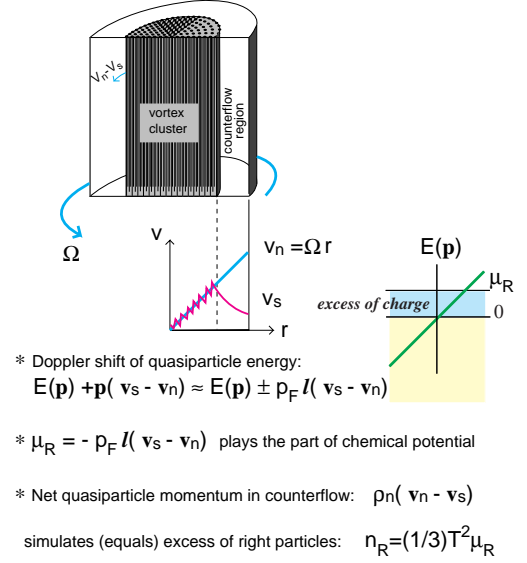


FIG. 7. The counterflow generated by the rotation of the cryostat is equivalent to the nonzero chemical potential for the right electrons. When the cryostat is rotating the typical situation is that the vortices form the vortex cluster in the center of the vessel. Within the cluster the average superfluid velocity  $\langle \mathbf{v}_s \rangle$  follows the solid-body-like rotation velocity of the normal component:  $\langle \mathbf{v}_s \rangle = \mathbf{v}_n = \boldsymbol{\Omega} \times \mathbf{r}$ . Outside the cluster the normal component performs the solid-body rotation, while the superfluid is irrotational. As a result one has the counterflow  $\mathbf{w} = \mathbf{v}_s - \mathbf{v}_n$  between the superfluid and normal components. In the counterflow region the  $\hat{\mathbf{l}}_0$ -vector is oriented along the counterflow. The Doppler shift of the quasiparticle energy plays the part of the chemical potential  $\mu_R$  and  $\mu_L$  for the chiral fermions in the vicinity of two gap nodes. In the counterflow the quasiparticles have net linear momentum. This excess of the fermionic charge of quasiparticles is equivalent to the excess of the chiral right-handed electrons if their chemical potential  $\mu_R$  is nonzero.

### B. Fermionic charge and Chern-Simons energy.

In the presence of counterflow,  $\mathbf{w} = \mathbf{v}_s - \mathbf{v}_n$ , of the superfluid component of  $^3\text{He-A}$  liquid with respect to the normal one, the energy of quasiparticles is Doppler shifted by the amount  $\mathbf{p} \cdot \mathbf{w}$ , which is  $\approx \pm p_F (\hat{\mathbf{l}}_0 \cdot \mathbf{w}_0)$  near the nodes. The counterflow therefore produces an effective chemical potentials for the relativistic fermions in the vicinity of both nodes (Fig. 7):

$$\mu_R = -p_F (\hat{\mathbf{l}}_0 \cdot \mathbf{w}_0), \quad \mu_L = -\mu_R \quad (47)$$

According to our analogy the relevant fermionic charge of our system, which is anomalously conserved and which

corresponds to the number of right fermions, is quasi-particle momentum  $P$  along  $\hat{\mathbf{l}}$  divided by  $p_F$ . Since the quasiparticle momentum is  $\mathbf{P} = -n_{n\parallel} \mathbf{w}$  the fermionic charge is

$$\frac{P}{p_F} = -\frac{n_{n\parallel} \hat{\mathbf{l}}_0 \cdot \mathbf{w}_0}{p_F}. \quad (48)$$

Using Eq.(36) for  $n_{n\parallel}$ , Eq.(6) and Eq.(4) for the metric tensor and Eq.(47) for the chemical potential, one obtains a very simple covariant expression for fermionic charge

$$n_R \equiv \frac{P}{p_F} = \frac{1}{3} T^2 \mu_R \sqrt{-g}. \quad (49)$$

Here  $g$  is the determinant of the metric tensor  $g_{\mu\nu}$

$$\sqrt{-g} = \frac{1}{c_{\parallel} c_{\perp}^2} = \frac{m^* p_F}{\Delta_0^2}. \quad (50)$$

The Eq.(49) represents the number density of the chiral right-handed massless electrons induced by the chemical potential  $\mu_R$  at temperature  $T$ . This is a starting point of the Joyce-Shaposhnikov scenario of the magnetogenesis. It is assumed that at an early stage of the universe, possibly at the Grand Unification epoch ( $10^{-35}$  s after the big bang), an excess of chiral right-handed electrons,  $e_R$ , is somehow produced due to parity violation.

The equilibrium relativistic energy of the system of right electrons also appears to be completely equivalent to the kinetic energy of the quasiparticles in the counterflow in Eq.(40)

$$\epsilon_R = \frac{1}{6} T^2 \mu_R^2 \sqrt{-g} \equiv \frac{1}{2} m_3 n_{n\parallel} (\mathbf{w}_0 \cdot \hat{\mathbf{l}}_0)^2, \quad (51)$$

The difference in the sign between Eq.(40) and Eq.(51) is the usual difference between the thermodynamic potentials at fixed chemical potential and at fixed particle number (fixed velocity and fixed momentum correspondingly).

Due to the axial anomaly the leptonic charge (excess of right electrons) can be transferred to the ‘‘inhomogeneity’’ of the vacuum. This inhomogeneity, which absorbs the fermionic charge, arises as a hypermagnetic field configuration. So the charge absorbed by the hypermagnetic field,  $\nabla \times \mathbf{A}$ , can be expressed in terms of its helicity,

$$n_R \{\mathbf{A}\} = \frac{1}{2\pi^2} \mathbf{A} \cdot (\nabla \times \mathbf{A}). \quad (52)$$

The right-hand side is the so called Chern-Simons (or topological) charge of the magnetic field.

When this charge is transformed from the fermions to the hypermagnetic field, the energy sitting in the fermionic system decreases. This leads to the gain in the energy, which is equal to the Chern-Simons charge multiplied by the chemical potential:

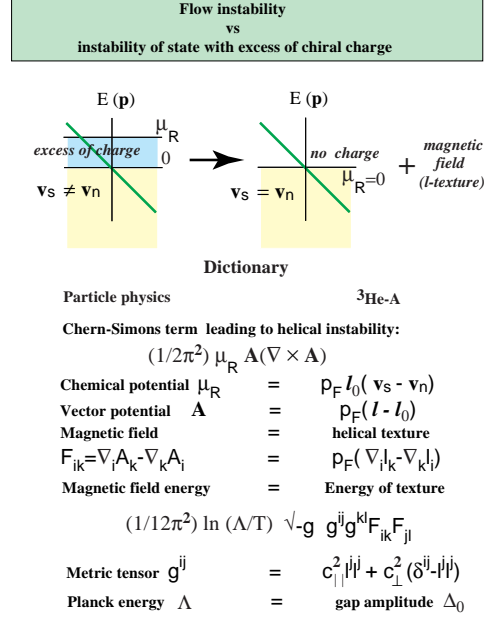


FIG. 8. The excess of the chiral right-handed electrons in early Universe can be effectively converted to the hypermagnetic field due to the mechanism of chiral anomaly. This is described essentially by the same equations as the counterflow instability observed in <sup>3</sup>He-A.

$$F_{CS} = n_R \{\mathbf{A}\} \mu_R = \frac{1}{2\pi^2} \mu_R \mathbf{A} \cdot (\nabla \times \mathbf{A}). \quad (53)$$

The translation to the <sup>3</sup>He-A language according to the dictionary in Fig. (8) gives the following energy change when the texture is formed from the counterflow

$$F_{CS} = \frac{p_F^3}{2\pi^2} (\hat{\mathbf{l}}_0 \cdot \mathbf{w}_0) (\delta \hat{\mathbf{l}} \cdot \nabla \times \delta \hat{\mathbf{l}}). \quad (54)$$

This exactly coincides with Eq.(42).

The Chern-Simons term in Eqs.(53,54) can have an arbitrary sign: it is positive if the counterflow is increased and negative if the counterflow is reduced. Thus one can have an energy gain from the transformation of the counterflow (fermionic charge) to the texture (hypermagnetic field). This energy gain is however confronted by the positive energy terms in Eq.(41) and Eq.(43). Let us consider these two terms in more detail.

### C. Maxwell Lagrangian for hypermagnetic and hyperelectric fields.

The Lagrangian for  $\delta \hat{\mathbf{l}}$ -texture in Eq.(41) is completely equivalent to the conventional Maxwell Lagrangian for the (hyper) magnetic and electric fields. For example the textural energy being written in the covariant form corresponds to the magnetic energy:

$$F_{\text{magn}} = \ln \left( \frac{\Delta_0^2}{T^2} \right) \frac{p_F^2 v_F}{24\pi^2 \hbar} (\partial_z \delta \hat{\mathbf{l}})^2 \quad (55)$$

$$\equiv \frac{\sqrt{-g}}{2\gamma^2} g^{ij} g^{kl} F_{ik} F_{jl} \quad (56)$$

Here  $F_{ik} = \nabla_i A_k - \nabla_k A_i$ , and  $\gamma^2$  is the running coupling, which is logarithmically diverges due to the vacuum polarization:

$$\gamma^{-2} = \frac{1}{12\pi^2} \ln \left( \frac{\Delta_0^2}{T^2} \right) \quad (57)$$

The Eq.(56) transforms to Eq.(55) if one takes into account that in our geometry the "hypermagnetic" field  $\mathbf{B} \perp \hat{\mathbf{l}}_0$ .

The gap amplitude  $\Delta_0$ , the ultraviolet cut-off in the logarithmically divergent magnetic energy, plays the part of the Planck energy scale. Note that  $\Delta_0$  has a parallel with the Planck energy in some other situations also. For example the analog of cosmological constant, which arises in the effective gravity of  ${}^3\text{He-A}$ , has the value  $\Delta_0^4/12\pi^2$  [41].

#### D. Mass of hyperphoton.

The "hyperphoton" in  ${}^3\text{He-A}$  has a mass. There are several sources of this mass.

(i) The mass of the "hyperphoton" comes from in Eq.(43), when it is written in the covariant form:

$$F_{\text{mass}}(T, \mu_R) = \frac{1}{6} \sqrt{-g} g^{ik} A_i A_k \frac{T^2 \mu_R^2}{\Delta_0^2} \quad (58)$$

It corresponds to the mass

$$M_{ph}^2 = \frac{\gamma^2}{3} \frac{T^2 \mu_R^2}{\Delta_0^2} \quad (59)$$

which appears due to the finite  $T$  and finite  $\mu_R$ . In  ${}^3\text{He-A}$  this mass is physical, though it contains the "Planck" energy cut-off  $\Delta_0$ : the "hyperphoton mass" is the gap in the spectrum of the orbital waves, propagating oscillations of  $\delta \hat{\mathbf{l}}$ , which correspond to the hyperphoton. This mass appears due to the presence of the counterflow, which provides the restoring force for oscillations of oscillations of  $\delta \hat{\mathbf{l}}$ . In the relativistic counterpart of  ${}^3\text{He-A}$ , the corresponding mass of hyperphoton disappears in the limit of the infinite cut-off parameter or is small, if the cut-off is of Planck scale.

(ii) In the collisionless regime  $\omega\tau \gg 1$ , the nonzero mass term appears even in the absence of the counterflow  $\mathbf{w}$ . It corresponds to the high-frequency photon mass in the relativistic plasma calculated by Weldon [42]:

$$M_{ph}^2(\omega\tau \gg 1) = \frac{N_F}{18} \gamma^2 T^2 \quad (60)$$

Here  $N_F$  is the number of fermionic species and  $\gamma$  again is the running coupling. This can be easily translated to the  ${}^3\text{He-A}$  language, since the mass is the covariant quantity. Substituting the running coupling from Eq.(57) and taking into account that the number of the fermions in  ${}^3\text{He-A}$  is  $N_F = 2$ , one obtains the gap in the high-frequency orbital waves (called also the normal flapping mode)

$$M_{\text{orb waves}}^2(\omega\tau \gg 1) = \frac{4\pi^2}{3} \frac{T^2}{\ln(\Delta_0^2/T^2)} \quad (61)$$

This coincides with the Eq.(11.76b) of [39] for the normal flapping mode. Note that in  ${}^3\text{He-A}$  this gap in the spectrum, corresponding to the relativistic plasma oscillations, was obtained by Wölfle already in 1975 [43].

The corresponding mass term in the Lagrangian for the gauge bosons is

$$F_{\text{mass}}(T, \omega\tau \gg 1) = \frac{N_F}{36} T^2 \sqrt{-g} g^{ik} A_i A_k \quad (62)$$

which is valid both for the relativistic theory with chiral fermions and for  ${}^3\text{He-A}$ , where  $N_F = 2$ .

There are also (iii) The topological mass of the "photon" in  ${}^3\text{He-A}$ , which comes from the axial anomaly and intrinsic angular momentum [12,44,45]. It is rather small. (iv) The mass coming from the spin-orbital interaction in  ${}^3\text{He-A}$  [45] described by the energy term [39]

$$-g_D (\hat{\mathbf{l}} \cdot \hat{\mathbf{d}})^2, \quad (63)$$

where  $\hat{\mathbf{d}}$  is the unit vector of the spontaneous anisotropy in spin space.

#### E. Instability towards magnetogenesis.

For us the most important property of axial anomaly term in Eqs.(53,54) is that it is linear in the derivatives of  $\delta \hat{\mathbf{l}}$ . Its sign thus can be negative, while its magnitude can exceed the positive quadratic term in eq. (55). This leads to the helical instability towards formation of the inhomogeneous  $\delta \hat{\mathbf{l}}$ -field. During this instability the kinetic energy of the quasiparticles in the counterflow (analog of the energy sitting in the fermionic degrees of freedom) is converted into the energy of inhomogeneity  $\nabla_z \delta \hat{\mathbf{l}}$ , which is the analog of the magnetic energy of the hypercharge field.

This instability can be found by investigation of the eigen values of the quadratic form describing the energy in terms of  $\mathbf{A} = p_F \delta \hat{\mathbf{l}}$  in Eqs.(41-43). Using the covariant form of these equations one obtains the following  $2 \times 2$  matrix for two components of the vector potential,  $A_x = A_{x0} e^{iqz}$  and  $A_y = A_{y0} e^{iqz}$ :

$$\begin{pmatrix} M_{ph}^2 + c_{\parallel}^2 q^2 & \frac{\gamma^2}{2\pi^2} \mu_R c_{\parallel} q \\ \frac{\gamma^2}{2\pi^2} \mu_R c_{\parallel} q & M_{ph}^2 + c_{\parallel}^2 q^2 \end{pmatrix} \quad (64)$$

This matrix is applied both to Joyce-Shaposhnikov scenario and to instability of the  $^3\text{He-A}$  superflow. This is one of the rare cases when the equation of motion for  $\hat{\mathbf{l}}$ -vector reduces to relativistic (Maxwell + Chern-Simons) equations. This comes from the fact that for the investigation of the stability one needs the energy, which is quadratic in terms of the small deviations of the vector potential (vector  $\hat{\mathbf{l}}$ ) from the uniform background. In our geometry: (i) The equilibrium unit vector  $\hat{\mathbf{l}}_0$  is oriented in one direction (along the velocity), which means that the background metric is constant in space. (ii) Small deviations  $\delta\hat{\mathbf{l}} \equiv \mathbf{A}/p_F$  of vector  $\hat{\mathbf{l}}$  from equilibrium are perpendicular to the flow, while the relevant coordinate dependence (i.e. which leads to instability) is the  $z$  dependence along the flow. Thus there are no derivatives in  $x$  and  $y$  in the relevant Lagrangian, while  $\mathbf{A}$  contains only the transverse components. (iii) The Lagrangian is quadratic in gauge field  $\mathbf{A} \equiv p_F\delta\hat{\mathbf{l}}$ , while the metric enters only as a constant (though anisotropic) background. All these conspire to produce the complete analogy with the relativistic theory. Such geometry, in which the analogy is exact, is really unique, and it is a miracle, that it can occur in a real experimental situation.

The quadratic form in Eq.(64) becomes negative if

$$\frac{\mu_R}{M_{ph}} > \frac{4\pi^2}{\gamma^2}, \quad (65)$$

Inserting the photon mass from Eq.(59) one finds that the uniform counterflow becomes unstable towards the nucleation of the texture if

$$\frac{T}{\Delta_0} \ln^{1/2} \left( \frac{\Delta_0^2}{T^2} \right) < \frac{3}{2\pi}, \quad (66)$$

If this condition is fulfilled, the instability occurs for any value of the counterflow (any value of the chemical potential  $\mu_R$  of right electrons).

In the relativistic theories, where  $\Delta_0$  is the Planck energy, this condition always fulfils, thus the excess of the fermionic charge is always unstable towards nucleation of the hypermagnetic field. This instability represents the scenario of the magnetogenesis developed by Joyce and Shaposhnikov [35,36]. The hypermagnetic field formed during this instability transforms finally to the electromagnetic magnetic field after electroweak symmetry breaking.

In  $^3\text{He-A}$  the instability occurs only if the temperature is low enough compared to  $\Delta_0$  ( $\Delta_0 \sim 2T_c$  [39]). In our analysis we used the limit  $T \ll \Delta_0$ , that is why the condition (66) is very approximate. In the rigorous theory, which holds at any  $T$ , the counterflow is unstable if  $T < 0.8T_c$  (see Sec. 7.10.1 in the book [39]). The counterflow instability in  $^3\text{He-A}$  has been intensively discussed theoretically (see e.g. [46]).

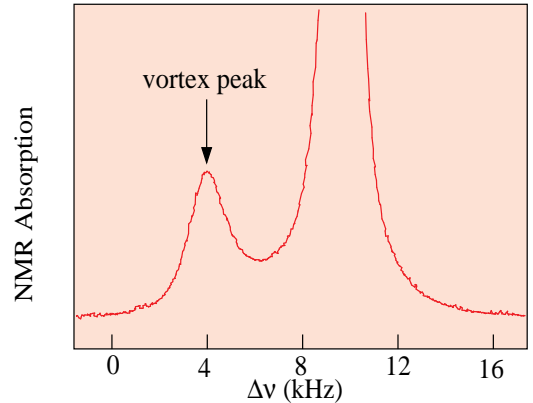


FIG. 9. The NMR signal from array of ATC vortices in the container. The position of the satellite peak indicates the type of the vortex, while the intensity is proportional to the number of vortices in the cell.

### F. "Magnetogenesis" in $^3\text{He-A}$ .

In real experiments [37,47,38] the flow instability is measured using the NMR technique, which means that one needs an external (real) magnetic field  $\mathbf{H}$ . Such field adds an additional mass to the "hypercharge gauge field"  $\mathbf{A}$  due to the spin-orbital interaction in Eq.(63). As a result even at low  $T$  the instability occurs only above some critical value of the counterflow velocity  $w_0$  (or corresponding chemical potential of right electrons  $\mu_R$ ). The critical value  $\mu_R^{cr}$  depends on  $T$  and  $H$ .

When this helical instability develops in  $^3\text{He-A}$ , the final result must be the formation of such  $\hat{\mathbf{l}}$ -texture, which corresponds to the free energy minimum in the rotating vessel. This is the periodic  $\hat{\mathbf{l}}$ -texture, which elementary cell represents the so-called Anderson-Toulouse-Chechetkin (ATC) continuous vortex (see Fig. 9(a)). The presence of ATC vortices and their number are extracted from the NMR absorption line, which contains the satellite peaks coming from different types of vortices [48]. The position of the satellite peak indicates the type of the vortex, while the intensity is proportional to the number of vortices in the cell. The corresponding satellite peak for the ATC vortices is shown on Fig. 9(b)).

In the Helsinki experiment the initial state did not contain vortices. Then the vessel was put into rotation with some angular velocity  $\Omega$ . If the velocity is small enough, one has the counterflow and no vortex texture. This means that there is a nonzero "chemical potential of right electrons",  $\mu_R = p_F\Omega r$ , where  $r$  is the distance from axis of rotating vessel, while the "hypermagnetic" field is absent. Accelerating the vessel further one finally reaches the critical value  $\mu_R^{cr}$  at the vessel wall,  $r = R$ , where the counterflow is maximal. At this moment the instability occurs, which is observed by the Helsinki group as jump in the height of the vortex peak (see Fig. 10). The peak

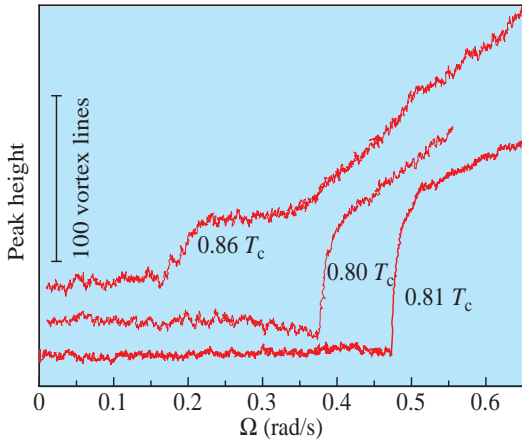


FIG. 10. Time dependence of the peak height of the continuous vortices. Initially vortices are not present in the vessel. When the velocity of the counterflow  $\mathbf{w}$  in the  $\hat{\mathbf{l}}_0$  direction (corresponding to the chemical potential  $\mu_R$  of the chiral electrons) exceeds some critical value, the instability occurs and the container becomes filled with the  $\hat{\mathbf{l}}$ -texture (hypermagnetic field) forming the vortex array.

height jumps from zero to the magnitude corresponding to almost equilibrium vortex array, which fills almost all the cell. This means that the counterflow was essentially reduced. The large amount of the counterflow (fermionic charge) was thus converted to the  $\hat{\mathbf{l}}$ -texture (hypermagnetic field).

The magnitude of  $\mu_R^{cr}$  found from experiments [37] was in good quantitative agreement with the theoretical estimation of the mass of the “hyperphoton” determined by the spin-orbit interaction in Eq.(63). Thus the Helsinki experiments model the nucleation of the hypermagnetic field for different masses of the “hyperphoton”. They have also observed the flow instability in the limit when the contribution to the “hyperphoton” mass from the real external magnetic field  $H$  is zero: first the field  $H$  was turned off and after the instability had occurred the field was switched on again and the created “hypermagnetic field” was measured. In this case it was observed that  $\mu_R^{cr}$  was essentially reduced.

## V. AXION IN $^3\text{HE-A}$ .

We discussed how the quasiparticles and the  $\hat{\mathbf{l}}$ -texture can exchange the fermionic charge – the linear momentum – due to axial anomaly. There is another phenomenon: the  $\hat{\mathbf{l}}$ -texture and the moving superfluid vacuum can also exchange the momentum. Thus the  $\hat{\mathbf{l}}$ -texture serves as an intermediate object which allows to transfer the fermionic charge from the condensate (vacuum) motion to the quasiparticles (matter), as was discussed in Sec.2C. In this sense the  $\hat{\mathbf{l}}$ -texture plays the

same role as quantized vortices in superfluids and superconductors. This again shows the common properties of continuous  $\hat{\mathbf{l}}$ -textures (with continuous vorticity) and quantized vortices, which are related to the gap nodes: In the  $\hat{\mathbf{l}}$ -textures the gap nodes are in the momentum space, while in quantized vortices of conventional superconductors and also in cosmic strings the nodes are in real space – in the cores of vortices, where the symmetry is restored and fermions are massless. The transformation between the momentum-space and real-space zeroes and the relation of both types of zeroes to axial anomaly were discussed in [49].

Let us now consider the exchange between the superfluid vacuum and the texture. The momentum density of the superfluid vacuum along the equilibrium  $\hat{\mathbf{l}}_0$ -vector is  $m_3 n_3 v_{sz}$ . The momentum exchange follows from the anomalous nonconservation of the momentum Eq.(22):

$$m_3 n_3 (\partial_t v_{sz} + \partial_z \mu_3) = \frac{p_F}{2\pi^2} (\partial_t \mathbf{A} \cdot \nabla \times \mathbf{A}) . \quad (67)$$

where  $\mu_3$  is the real chemical potential of  $^3\text{He}$  atoms, which also determines the speed of sound in  $^3\text{He-A}$ :  $s^2 = n_3 d\mu_3 / dn_3$ ;  $\mathbf{A} = p_F \delta \hat{\mathbf{l}}$ ; and we consider only the  $z$ - and  $t$ -dependence of all variables.

Let us now introduce the variable which is dual to the potential  $\phi$  of the flow:

$$\partial_t \theta = -\frac{p_F}{2m_3} \partial_z \phi = -p_F v_{sz} , \quad (68)$$

$$\partial_z \theta = -\frac{p_F}{2m_3 s^2} \partial_t \phi = \frac{p_F}{s^2} \delta \mu_3 , \quad (69)$$

Now one can write the Lagrangian which variation gives rise to the anomalous nonconservation of the condensate momentum in Eq.(67):

$$\frac{1}{2\pi^2} \theta \left( \partial_t \vec{A} \cdot \vec{\nabla} \times \vec{A} \right) + \frac{n_3 m_3}{2p_F^2} (s^2 (\partial_z \theta)^2 - (\partial_t \theta)^2) . \quad (70)$$

This is nothing but the action for the axion field  $\theta$ , which interacts with the CP violated combination  $F^{\mu\nu} \tilde{F}_{\mu\nu} \propto \mathbf{E} \cdot \mathbf{B}$  [50].

In  $^3\text{He-A}$  the axion corresponds to sound waves – propagating oscillations of two conjugated variables, the phase  $\phi$  and the particle density  $n_3$ . The anomalous first term in Eq.(70) can be also obtained from Eq.(46). The speed of sound is  $s^2 = (1/3) v_F^2 (1 + F_0)(1 + F_1/3)$ , where  $F_0$  and  $F_1$  are the Fermi-liquid parameters, and it is the same in the superfluid  $^3\text{He-A}$  ( $T < T_c$ ) and in the normal liquid  $^3\text{He}$  above the superfluid transition temperature  $T > T_c$ . As distinct from the orbital waves (“electromagnetic waves”), the speed of sound waves does not coincide with any of two speeds of light,  $c_\perp$  and  $c_\parallel$ , though one can expect that the axion propagating along  $z$  must have the parallel speed of “light”  $c_\parallel = v_F$ . What is the reason? This is the property of the superfluid  $^3\text{He-A}$ :

Both modes, "photon" (orbital wave) and "axion" (sound wave) are collective bosonic excitations of the fermionic system and are obtained by integration over the fermions. In the case of "photons" the relevant region of the integration over the fermions is concentrated close to the gap nodes due to logarithmic divergency. Near the nodes the fermions are relativistic and are described by the Lorentzian metric  $g^{\mu\nu}$ . As a result, the effective "photons" are described by the same metric and therefore the speed of light is the same as the speed of the massless fermion propagating in the same direction.

On the contrary, the relevant region of the integration, which is responsible for the spectrum of the "axion" mode, is far from the gap nodes. As a result the axion spectrum even does not depend on the existence of the gap nodes.

## VI. DISCUSSION

In principle one can introduce the model system with favourable parameters, where for all the collective modes the integration over the fermions is concentrated mostly in the region where the fermions are Lorentzian. In this case the low-energy dynamics of photons, axions, gravitons, etc., will be determined by the same Lorentzian metric as fermions. So, in the low-energy corner one obtains the effective relativistic quantum field theory and the effective quantum gravity with the same speed of light for all bosons and fermions.

It is interesting that in this ideal case the cosmological constant will vanish in this effective theory. This follows from the fact that the Eq.(3) for the spectrum of massless quasiparticles can be multiplied by arbitrary factor  $a^2$ , which does not change the energy spectrum, but changes the contravariant metric tensor:  $g^{\mu\nu} \rightarrow a^2 g^{\mu\nu}$ . Since the physics cannot depend on such formal conformal transformation, the effective low-energy Lagrangian for the gravity cannot depend on  $a^2$  and thus the cosmological term  $\int d^3x dt \Lambda \sqrt{-g}$  is prohibited (on the discussion of the role of the scale invariance in the vanishing of the cosmological constant see [51]). This situation is somewhat similar to that which occurs in the normal Fermi-liquid where the role of the parameter  $a^{-1}$  is played by the quasiparticle spectral weight  $Z$  – the residue of the Green's function at the quasiparticle pole. The low-energy properties of this system, described by the Landau phenomenological Fermi-liquid theory, do not depend on  $Z$ .

The effective low-energy electrodynamics and quantum gravity follow from existence of the gap nodes in the fermionic spectrum and from the dynamics of the node. The fundamental constants in these effective theories are determined by the position of the node,  $p_F$ , and by the slopes of the energy  $E$  of the quasiparticle as a function of its momentum  $\mathbf{p}$  at the node. There are three such

parameters in  $^3\text{He-A}$ : the Fermi velocity  $v_F$ , the Fermi momentum  $p_F$  and the gap amplitude  $\Delta_0$ . They give: the parallel speed of light  $c_{\parallel} = v_F$ ; the transverse speed of light  $c_{\perp} = \Delta_0/p_F$ ; the Planck energy  $\Delta_0$ ; the running coupling in Eq(57); the masses of the hyperphoton in Eqs.(59,60); cosmological and gravitation constants  $\Delta_0^4/12\pi^2$  and  $\pi/(2\Delta_0^2)$  correspondingly; etc.

We discussed only 3 experiments in superfluid  $^3\text{He-A}$  related to the properties of the electroweak vacuum. In all of them the chiral anomaly is an important mechanism. It regulates the nucleation of the fermionic charge from the vacuum as was observed in Manchester [26] and the inverse process of the nucleation of the effective magnetic field from the fermion current as was observed in Helsinki [37,38].

There are many other connections between the superfluid  $^3\text{He}$  and different branches of physics which should be exploited. For example, we can simulate the phenomena related to the effective gravity, such as cosmological constant, quantum properties of event horizon, vacuum instability in strong gravity, torsion strings and even inflation. In principle the nonequilibrium vacuum state can be constructed in which the speed of light  $c_{\perp} = \Delta_0/p_F$  decreases exponentially with time. In the cosmological language this would mean the inflation, since the length scale in the space metric  $g_{ik}$  is growing exponentially. This will allow us to study the development of perturbations during inflation.

Till now we considered the properties related to one pair of nodes only. If one takes into account that in  $^3\text{He-A}$  there are two Fermi surfaces (sheets) corresponding to two spin projection of the  $^3\text{He}$  atom, the number of fermionic and bosonic degrees of freedom increases. It appears that with these new degrees of freedom, the system transforms to the  $SU(2)$  gauge theory: the conventional spin degrees of freedom of  $^3\text{He}$  atoms form the  $SU(2)$  isospin, while some collective modes of the order parameter (the spin-orbital waves) behave as  $SU(2)$  gauge bosons [12].

There are several ways of extension of the model, in which the higher local and global symmetry groups can naturally arise. (1) One can imagine the initial normal state of condensed matter consisting of 3,4, etc. sheets of the Fermi-surface, which can give rise to higher gauge group:  $SU(3)$ ,  $SU(4)$ , etc. (2) The number of gap nodes on each Fermi-surface can be also larger than 2. For example the so called  $\alpha$ -state of  $^3\text{He}$  [39] contains 8 gap nodes per Fermi-surface and thus 8 elementary relativistic fermions in the vicinity of the nodes. The fluctuations of positions of these nodes are equivalent to several gauge fields. In high- $T_c$  superconductivity each Fermi-sheet (actually the Fermi-circle since the superconductivity effectively occurs in 2D space of CuO plane) contains 4 gap nodes. The corresponding Weyl-like Hamiltonian for 4 fermions and the corresponding gauge fields have been discussed for this material [52]. So in principle one

can construct the model, which has as many fermionic and bosonic degrees of freedom as GUT + gravity. Of course, the construction of the proper condensed matter corresponding to such a model is not an easy task.

## VII. ACKNOWLEDGEMENTS

I thank Uwe Fischer, Henry Hall, John Hook, Ted Jacobson, Michael Joyce, Tom Kibble, Matti Krusius, Robert Laughlin, Misha Shaposhnikov, Tanmay Vachaspati and Shuqian Ying for fruitful discussions.

- 
- [1] F. Wilczek, "The Future of Particle Physics as a Natural Science", hep-ph/0702371
- [2] H.B. Nielsen, "Field theories without fundamental (gauge) symmetries", preprint NBI-HE-83-41.
- [3] A.D. Sakharov, Sov. Phys. Doklady **12**, 1040 (1968).
- [4] Ya.B. Zeldovich, "Interpretation of electrodynamics as a consequence of quantum theory", Pis'ma ZhETF **6**, 922-925 (1967) [JETP Lett. **6** 345-347 (1967)].
- [5] R. Laughlin, "Gauge Theories from Nothing in Condensed Matter: Are Quantum Critical Points Supersymmetric Field Theories", the talk at symposium on QUANTUM PHENOMENA at LOW TEMPERATURES, Helsinki, 7-11 January, 1998.
- [6] G.E. Volovik, "Simulation of Quantum Field Theory and Gravity in Superfluid He-3", cond-mat/9706172.
- [7] T. Jacobson and G.E. Volovik, "Event horizons and ergoregions in  $^3\text{He}$ ," cond-mat/9801308.
- [8] N. B. Kopnin and G. E. Volovik, "Rotating vortex core: An instrument for detecting the core excitations," cond-mat/9706082.
- [9] W.G. Unruh, Phys. Rev. Lett. **46** 1351 (1981); Phys. Rev. **D 51** 2827 (1995).
- [10] T. Jacobson, Phys. Rev. **D 44** 1731 (1991).
- [11] M. Visser, "Acoustic black holes: horizons, ergospheres, and Hawking radiation", gr-qc/9712010.
- [12] G.E. Volovik, Exotic properties of superfluid  $^3\text{He}$ , World Scientific, Singapore-New Jersey-London-Hong Kong, 1992.
- [13] G.E. Volovik and T. Vachaspati, "Aspects of  $^3\text{He}$  and the standard electroweak model", Int. J. Mod. Phys. **B 10**, 471-521 (1996).
- [14] S.H. Simon and P.A. Lee, Phys. Rev. Lett., **78**, 1548 (1997); **78**, 5029 (1997).
- [15] X.G. Wen, Phys. Rev. B, **43**, 11025 (1991)
- [16] M. Stone, Annals of Phys., **207**, 38 (1991).
- [17] R.B. Laughlin, "Magnetic Induction of d + i d Order in High-Tc Superconductors", cond-mat/9709004.
- [18] G.E. Volovik, "On edge states in superconductor with time inversion symmetry breaking", JETP Lett. **66**, 522-527 (1997).
- [19] S. Ying, "The Quantum Aspects of Relativistic Fermion Systems with Particle Condensation", hep-th/9711167;
- M. Alford, K. Rajagopal, F. Wilczek, "QCD at Finite Baryon Density: Nucleon Droplets and Color Superconductivity", hep-ph/9711395.
- [20] S. Adler, Axial-vector vertex in spinor electrodynamics, Phys. Rev. **177**, 2426-2438 (1969).
- [21] J.S. Bell and R. Jackiw, A PCAC puzzle:  $\pi^0 \rightarrow \gamma\gamma$  in the  $\sigma$ -model, Nuovo Cim. **A60**, 47-61 (1969).
- [22] V.R. Chechetkin, JETP, **44**, 706 (1976).
- [23] P.W. Anderson and G. Toulouse, Phys. Rev. Lett., **38**, 508 (1977).
- [24] G.E. Volovik, "Hydrodynamic Action for Orbital and Superfluid Dynamics of  $^3\text{He-A}$  at  $T = 0$ ", JETP **75**, 990 (1992).
- [25] N.B. Kopnin, Phys. Rev. **B 47**, 14354 (1993).
- [26] T.D.C. Bevan, A.J. Manninen, J.B. Cook, J.R. Hook, H.E. Hall, T. Vachaspati and G.E. Volovik, Momentogenesis by  $^3\text{He}$  vortices: an experimental analogue of primordial baryogenesis, Nature, **386**, 689-692 (1997).
- [27] T.D.C. Bevan, A.J. Manninen, J.B. Cook, H. Alles, J.R. Hook, H.E. Hall, Vortex mutual friction in superfluid  $^3\text{He}$  vortices, J. Low Temp. Phys. **109**, 423 - 459 (1997).
- [28] A.D. Dolgov, Rep. Prog. Phys., **222**, 309-386 (1992).
- [29] N. Turok, in Formation and interaction of topological defects, eds. A.C. Davis, R. Brandenberger (Plenum Press, New York, London), 1995, pp. 283-301.
- [30] E. Witten, Nucl. Phys. **B249**, 557-592 (1985).
- [31] T. Vachaspati and G.B. Field, Electroweak string configurations with baryon number, Phys. Rev. Lett. **73**, 373-376 (1994); **74**, 1258(E) (1995).
- [32] J. Garriga and T. Vachaspati, Zero modes on linked strings, Nucl. Phys. **B438**, 161-181 (1995).
- [33] M. Barriola, Phys. Rev. **D51**, 300-304 (1995).
- [34] G.D. Starkman, Phys. Rev. **D53**, 6711-6714 (1996).
- [35] M. Joyce, M. Shaposhnikov, Primordial magnetic fields, right electrons, and the abelian anomaly, Phys. Rev. Lett., **79**, 1193-1196 (1997).
- [36] M. Giovannini and E.M. Shaposhnikov, Primordial hypermagnetic fields and triangle anomaly, hep-ph/9710234.
- [37] V.M.H. Ruutu, J. Kopu, M. Krusius, U. Parts, B. Plaaais, E.V. Thuneberg, and W. Xu, Critical Velocity of Vortex Nucleation in Rotating Superfluid  $^3\text{He-A}$ , Phys. Rev. Lett., **79**, 5058 (1997).
- [38] M. Krusius, T. Vachaspati and G.E. Volovik "Flow instability in  $^3\text{He-A}$  as analog of generation of hypermagnetic field in early Universe," cond-mat/9802005.
- [39] D. Vollhardt, P. and P. Wölfle, The superfluid phases of helium 3, Taylor and Francis, London - New York - Philadelphia, 1990.
- [40] G.E. Volovik, "Orbital momentum of vortices and textures due to spectral flow through the gap nodes: Example of the  $^3\text{He-A}$  continuous vortex", JETP Lett. **61**, 958-964 (1995).
- [41] G.E. Volovik, "Analog of gravity in superfluid  $^3\text{He-A}$ ," JETP Lett. **44**, 498 - 501 (1986).
- [42] H.A. Weldon, Phys. Rev. **D 26**, 1394 (1982).
- [43] P. Wölfle, in "Quantum Statistics and the Many Body Problem" (S.B. Trickey, W.P. Kirk, and J.W. Duffy, Eds.) p.9. Plenum, New York, 1975.
- [44] G.E. Volovik, "Orbital momentum and orbital waves in the anisotropic A-phase of superfluid  $^3\text{He}$ ," JETP Lett.

- 22**, 108 - 110 (1975); "Dispersion of the orbital waves in the A-phase of superfluid  $^3\text{He}$ ," JETP Lett. **22**, 198 - 200 (1975).
- [45] A.J. Leggett and S. Takagi, "Orientational Dynamics of Superfluid  $^3\text{He}$ : A "Two-Fluid" Model. II. Orbital Dynamics", Ann. Phys. **110**, 353 - 406 (1978).
- [46] D. Vollhardt, "Stability of superflow and related textural transformations in superfluid  $^3\text{He}$ ", PhD Thesis, Hamburg, 1979.
- [47] V.M.H. Ruutu, V.B. Eltsov, A.J. Gill, T.W.B. Kibble, M. Krusius, Yu.G. Makhlin, B. Placais, G.E. Volovik and Wen Xu, Vortex formation in neutron irradiated  $^3\text{He}$  as an analogue of cosmological defect formation, Nature **382**, 334-336 (1996).
- [48] Ü. Parts, J.M. Karimäki, J.H. Koivuniemi, M. Krusius, V.M.H. Ruutu, E.V. Thuneberg, and G.E. Volovik, Phase diagram of vortices in superfluid  $^3\text{He}$ -A, Phys. Rev. Lett. **75**, 3320-3323 (1995).
- [49] G.E. Volovik, V.P. Mineev, "Current in superfluid Fermi liquids and the vortex core structure," JETP **56**, 579 - 586 (1982); G.E. Volovik, "Action for anomaly in fermi superfluids: quantized vortices and gap nodes", JETP **77**, 435 - 441 (1993).
- [50] M.S. Turner, "Windows on the axion", Phys. Rep. **197**, 67 (1990); J.E. Kim, "Cosmic Axion", astro-ph/9802061.
- [51] S.L. Adler, "A strategy for a vanishing cosmological constant in the presence of scale invariance breaking", Gen. Rel. Grav. **29** 1357-1362 (1997).
- [52] A.A. Nersisyan, A.M. Tselik and F. Wenger, Phys. Rev. Lett., **72**, 2628 (1994).